Top Quark Physics
(part 2)

S. Tokár, Comenius Univ., Bratislava
TES-HEP Summer School, Stará Lesná 2025
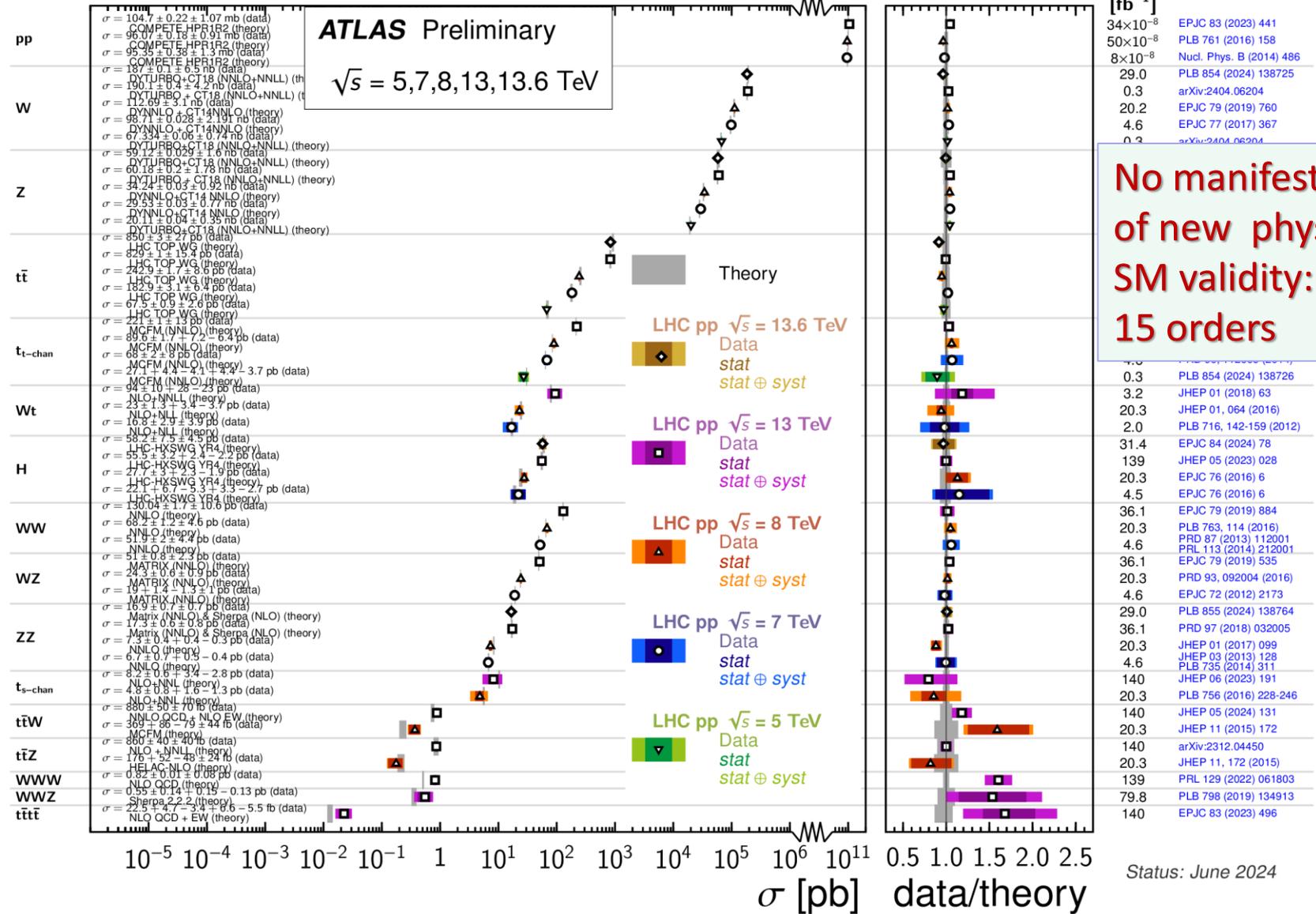
Topics in This Talk

➢ Top quark mass

➢ Top quark spin effects (top-antitop spin correlations)

➢ Quantum entanglement in top quark production

➢ Forward-backward /charge asymmetry

➢ Associated production of ttbar and gauge bosons (Z, W, γ)

➢ Flavor Changing Neutral Currents

SM vs LHC measurements: excellent agreement

Standard Model Total Production Cross Section Measurements

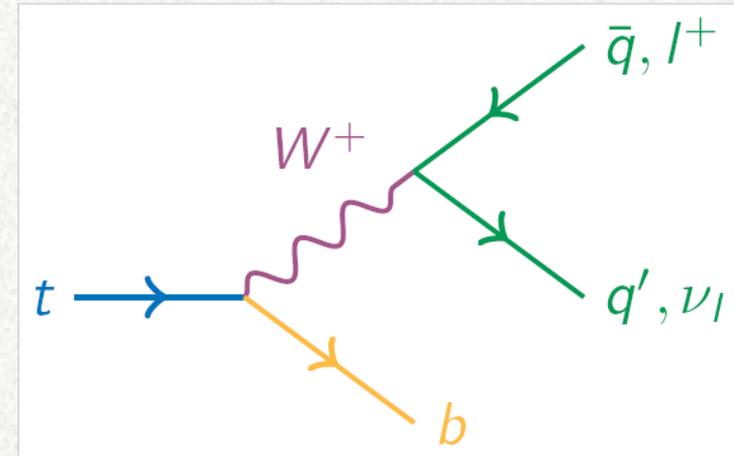No manifestation of new physics! SM validity: over 15 orders

Top Quark Mass

Top quark mass is very important parameter of the SM, in addition:

- ✓ Its role in consistency test of the SM.

- ✓ Electroweak vacuum stability.

- ✓ What is the top quark mass and how to measure it.

Top quark mass: Motivation

❑ The top quark mass (m_{top}) is one of the fundametal SM parameters.

❑ Its precise value provides a key input to global EW fit $\Rightarrow$ test of internal consistency of the SM.

❑ Its value leads to a significant constraints on stability of the EW vacuum.

❑ it has a significant impact on cosmological models with inflation-

❑ It looks the top quark mass can be easily determined using the top quark decay products – it is sufficient to measure **4-momentum of b quark** and 4-momenta of **W boson decay producs**:

$$\longrightarrow \quad m_{\text{top}}^2 = \left(E_W + E_b \right)^2 - \left(\vec{p}_W + \vec{p}_b \right)^2$$

… but there are some important ambiguities…

- Measured values of m_t, m_W & m_H can be compared to EW fit predictions to check validity of SM $\rightarrow$ higher order corrections to W/Z propagator leads to
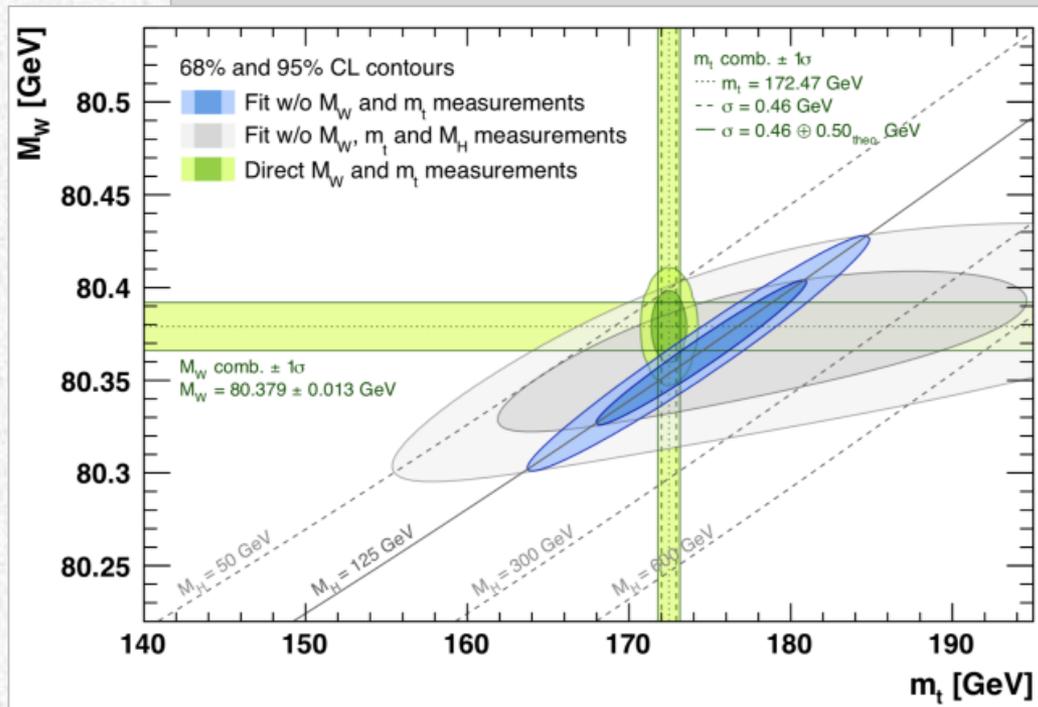
$$M_W^2\left(1 - \frac{M_W^2}{M_Z^2}\right) = \frac{\pi\alpha}{\sqrt{2}G_F}(1 + \Delta r), \quad \Delta r = \Delta\alpha + \frac{s_W}{c_W}\Delta\rho + (\Delta r)_{nl}$$

http://project-gfitter.web.cern.ch/project-gfitter/

$$\Delta\rho \sim m_t^2 \qquad (\Delta r)_{nl} \propto \ln M_H$$

A set of N_{exp} precisely measured observables described by N_{exp} theor. expressions with N_{mod} parameters

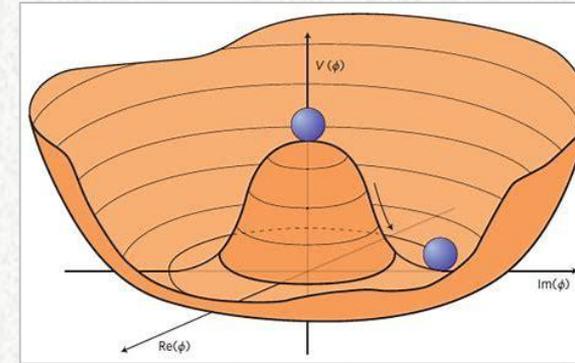Contours of 68% and 95% CL obtained from scans of fits with fixed variable pairs M_W vs m_t - Gfitter package used

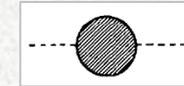Present status of the SM: high level of internal consistency !

LHC: **Higgs boson is firmly confirmed** $\Rightarrow$ under SM, vacuum has **non-zero component of Higgs field** (it is a Higgs condensate)

Higgs potential: $V(\phi) = \mu^2 \phi^* \phi + \lambda (\phi^* \phi)^2, \quad \phi = \dfrac{\phi_1 + i\phi_2}{\sqrt{2}}$

What can be said about its stability?

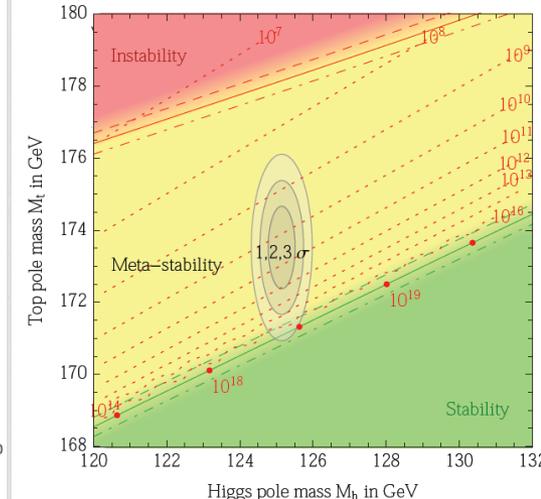for $\mu^2 < 0$ and $\lambda > 0$

Higgs boson is a dynamic object $\rightarrow$ quantum fluctuations $\Rightarrow \lambda$ is running constant depending on an energy scale :

$$\lambda(\mu_R) = \frac{G_F M_H}{\sqrt{2}} + \Delta\lambda(\mu_R)$$

present status: $T_{\text{vac}} \gg T_{\text{age}}$

✓ SM: $\Delta\lambda$ we can calculate it if there is no new physics

✓ What does it mean $\lambda < 0$?

Vacuum is metastable $\rightarrow$ tunneling from a local to absolute minimum!

3σ bands in
$M_t = 173.1 \pm 0.6$ GeV (gray)
$\alpha_3(M_Z) = 0.1184 \pm 0.0007$ (red)
$M_h = 125.7 \pm 0.3$ GeV (blue)

$M_t = 171.3$ GeV
$\alpha_s(M_Z) = 0.1205$
$\alpha_s(M_Z) = 0.1163$
$M_t = 174.9$ GeV

Instability
Meta–stability
1,2,3 σ
Stability

Precise values of M_{top}, M_H and α_S needed!

Degrassi et al., JHEP 1208 (2012) 098

Top-quark mass ambiguities

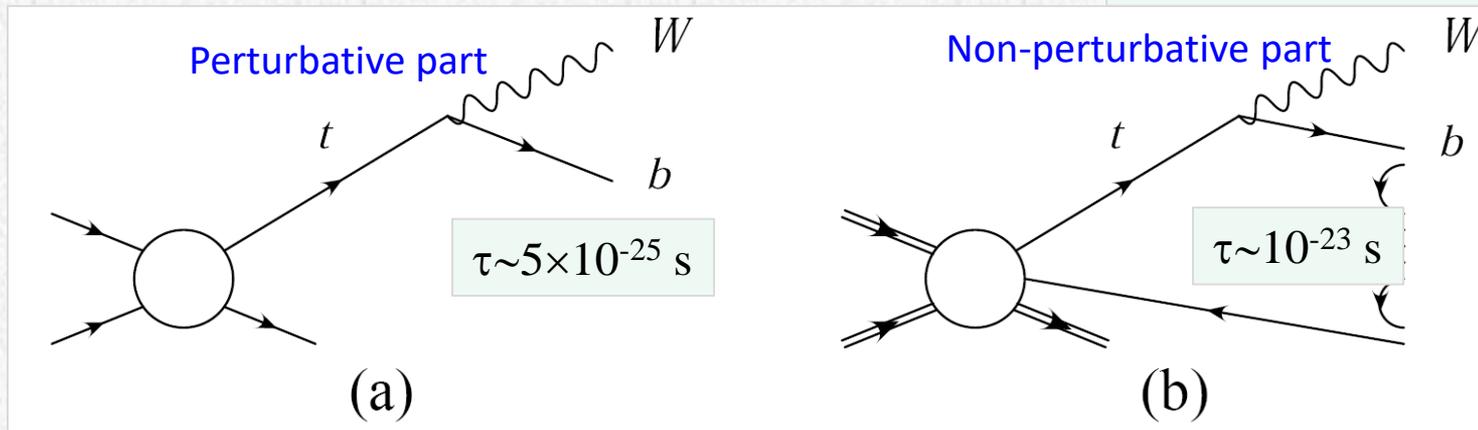Particle pole mass: corresponds to pole in propagator of „free" particle $\sim 1/(q^2 - m^2)$

The top quark pole mass (m^t_{pole}): top quark is a color object – due to confinement

the ambiguity of pole top mass is $\Delta m^t_{pole} \sim \Lambda_{QCD}$
$$\left(\alpha_S(Q^2) = \frac{4\pi}{\left(11 - \frac{2}{3}n_f\right)\ln\left(Q^2/\Lambda^2_{QCD}\right)} \right)$$

(a) Perturbative part — t, W, b; $\tau \sim 5 \times 10^{-25}$ s

(b) Non-perturbative part — t, W, b; $\tau \sim 10^{-23}$ s

Top quark pole mass is close to invariant mass of the top decay products.

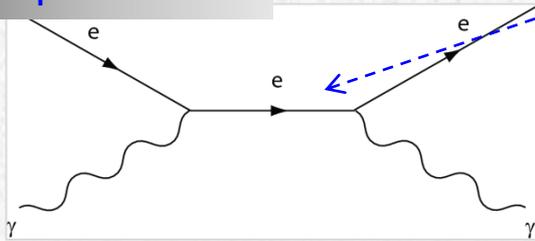Ambiguities are from: hadronization, color reconnection and extra radiation :

✓ at least one quark **not coming from top decay** is trapped by b-quark (non perturbative part).

✓ **Color reconnection**: the colored top quark decay product will interact with the colored rest of proton.

✓ **Extra radiation** from top decay products not included in reconstruction.

Particle mass – preliminary words
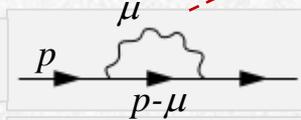
Let us start with electron

Compton effect

Electron propagator $\equiv \dfrac{i\left(\not p + m\right)}{p^2 - m^2 + i\varepsilon}$, $\quad \not p = p_\mu \gamma^\mu$ (1)

Electron mass = pole in electron propagator
$\rightarrow$ it is free-field propagator

→ divergent renormalization

Propagator correction:

Characterized by loop momentum μ or size $1/\mu$

Electron self energy: 1PI $\equiv$

Propagator in general:

$$\frac{i}{\not p - m_{pole}} = \frac{i}{\not p - m_0} + \frac{i}{\not p - m_0}\left(\frac{\Sigma(\not p)}{\not p - m_0}\right) + \frac{i}{\not p - m_0}\left(\frac{\Sigma(\not p)}{\not p - m_0}\right)^2 \cdots = \frac{i}{\not p - m_0 - \Sigma(\not p)} \quad (2)$$

bare mass

Other expansion: m_0 + all bubbles with size < $1/\mu_R$ are absorbed into mass $\longrightarrow$

$$\frac{i}{\not p - m_{pole}} = \frac{i}{\not p - m(\mu_R) - \Sigma(\mu_R, \not p)} \quad (3)$$

$m(\mu_R) \equiv$ short distance mass, $\Sigma \equiv$ self-energy: contribution of interactions to mass

Particle mass: top quark vs electron

Difference top quark *vs.* electron:

✓ top is unstable – pole is complex: $m_{top} + i\Gamma_{top}$

✓ Top is colored object - due to confinement its mass uncertainty $\sim \Lambda_{QCD}$

Top quark is not asymptotically free particle!

Top quark self energy Σ
in 1 loop approx.:

$$\Sigma^{(1)} = \quad \underset{p \quad\quad t \quad p\text{-}q}{\overbrace{\qquad\qquad}^{q}} \quad + \quad \underset{b}{\overbrace{\qquad\qquad}^{W}}$$

Loops need to be integrated over q (4-momentum conservation law: $p = q + (p\text{-}q)$ valid for all q).

$\Sigma^{(1)} = \int dq...$ diverges for $|q| \to \infty$ (UV divergence) $\Rightarrow$ removes by renormalization

for $|q| \to 0$ (IR divergence) $\Rightarrow$ top quark non-perturbativeness problems

Does not exist for electron

If loop size reaches a value $d \sim 1/\text{GeV}$, the coupling α_S gets big!

What is the Top Quark Mass ?

Introducing top quark short range mass, the top pole mass is

$$m_t^{\mathrm{pole}} = m_t^{\mathrm{MSR}}(R) + \Sigma^{\mathrm{fin}}(R,\mu) \qquad (7)$$

Absorbs bubbles with size > 1/R (problematic region) it contains perturbative and non-perturbative part

Absorbs all self energy bubbles

Absorbs self energy bubbles with size <1/R (perturb. region)

Relation between the **top-quark pole** and **short range mass**, $R\sim$1 GeV   PRL 117, 232001 (2016)

$$m_t^{\mathrm{pole}} - m_t^{\mathrm{MSR}}(R) = R\left(c_1 a + c_2 a^2 + c_3 a^3 + \ldots\right), a \equiv \alpha_S^{(5)}(R)/4\pi, c_1 = 5.33, c_2 = 131.79, c_3 = 4699.7$$

Advantage of short range mass: well defined mass from renormalization view point

✓ more stable in **perturbation theory** $\Rightarrow m_t^{\mathrm{MSR}}(R=1$ GeV) - close to the notion of kinematic mass, but no renormalon problems.

✓ A special case is $\overline{\mathrm{MS}}$ mass: $m_{t,\mathrm{MSR}}\left(R = \bar{m}(\bar{m})\right) = \bar{m}(\bar{m})$ $\Rightarrow$ it absorbs the self energy corrections $> \bar{m} \Rightarrow$ sensitive to only the short distance aspects of QCD.

Pole mass vs $\overline{\mathrm{MS}}$ mass perturbative expansion (4 loops approximation):

arXiv:1502.01030

$$m_t^{\mathrm{pole}} = \bar{m}(\bar{m})\left(1 + 0.4244\,\alpha_s + 0.8345\,\alpha_s^2 + 2.8345\,\alpha_s^3 + (8.49 \pm 0.25)\,\alpha_s^4 + \ldots\right) \qquad (8)$$

$$= 163.643 + 7.557 + 1.617 + 0.501 + 0.195 \pm 0.005 \text{ GeV}$$

$$\alpha_s \equiv \alpha_s^{(6)}(\bar{m}) = 0.1088$$

Short range mass vs reconstructed Top Quark Mass ?

How to relate the reconstructed top quark mass to short range or pole top quark mass?

MC event generators simulate:

Hard matrix element:

Initial parton annihilation and top production + additional hard partons from pQCD.

Parton shower evolution:

parton shower evolution describes the top decay products and continued splitting into higher multiplicity partonic states having subsequently lower virtualities.

Splitting probabilities from pQCD (valid to leading order for the top decay to an approximate leading logarithmic accuracy for soft-collinear splitting).

Can be viewed as a way to sum **dominant perturbative corrections** down to shower cut $\Lambda_s \approx 1$ GeV.

Hadronization model:

Turns partons into hadrons (**non-perturbative process**) - dependent on parton shower implementation.

Description of data (frequently) much better than the conceptual (LL) precision of parton evolution part.

How to measure top mass?

Top quark mass can be reconstructed in all $t\bar{t}$ topologies (LJ, DL AH)

Two basic mass determination approaches:

Direct measurements

✓ Extraction from total or partial kinematic reconstruction of invariant mass of top-quark decay products.

✓ Comparison with MC calculations of the "invariant mass" variable – MC templates.

 The result of comparison: m_t^{MC}.

Indirect measurements

✓ From cross-sections (inclusive or differential).

✓ Measuring observable(s) with a strong dependence on m_t with data unfolding m_t^{pole}
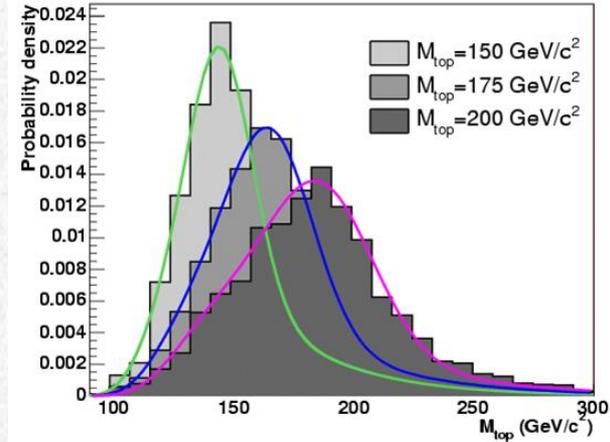
Top quark mass : kinematic approaches

Template method:

PRD 63, 032003(2001)

B-tagged signal templates

- ✓ uses **observable(s) sensitive to top quark mass** (e.g. invariant mass, m_t, of decay products).
- ✓ More than 1 observable can be used (to m_t also JES).
- ✓ Signal templates (for different m_{top}) + Bkgd one created by MC.
- ✓ Likelihood fit to data based on templates for S + B.

Matrix element method:

K. Kondo, J. Phys. Soc. Jap. 57, 4126 (1988).

evaluates **event-by-event probability** based on the full event kinematics

- ✓ signal probability:

measured 4-momenta   Matrix el.   partonic final-state 4-momenta

$$P_{t\bar{t}}\left(\vec{x};m_{top}\right) = \frac{1}{\sigma_{t\bar{t}}\left(m_{top}\right)} \sum_{\text{flavors}} \int dq_1 dq_2 d\vec{y} \, \frac{d\sigma\left(p\bar{p} \to t\bar{t} \to \vec{y}\right)}{d\vec{y}} \cdot f(q_1) f(q_2) \cdot W(\vec{x},\vec{y})$$

PDFs   resolution

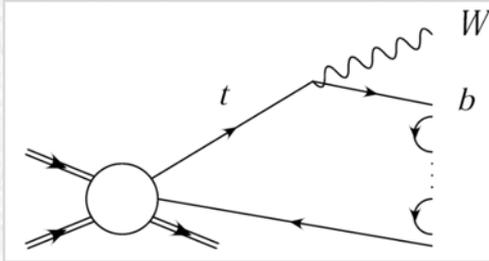- ✓ Top mass extracted from global likelihood fit to data based on P_{tt} **and** P_{bkg}

$$L\left(\vec{x}_1 \cdots \vec{x}_N; m_{top} \cdots\right) = \prod_{i=1}^{N}\left[f_t P_{tt}\left(\vec{x}_i; m_{top}\right) + \left(1 - f_t\right) P_{bkg}\left(\vec{x}_i\right) \right]$$

Other methods: combination of Template and Matrix element methods (ideogram m.)

Top-quark mass, kinematic approach

Top is a colored fermion – it decays before hadronization, the b quark from its decay hadronizes – it captures at least 1 quark from neighborhood.

Effect of b-hadronization on m_{top}:

$$\Delta m_{\text{top}} \sim \Lambda_{\text{QCD}} \approx 0.2\,\text{GeV}$$

ATLAS analysis (ATL-PHYS-PUB-2021-034):
Kinematic top mass vs MSR mass

$$m_t^{\text{MC}} = m_t^{\text{MSR}}\left(1\,\text{GeV}\right) + 80^{+350}_{-410}\,\text{MeV}$$

Relation between m_t^{MSR} and m_t^{pole} (top pole mass) in 4 loop approx.

$$\Rightarrow \quad m_t^{\text{MC}} = m_t^{\text{pole}} + 350^{+300}_{-360}\,\text{MeV}$$

PRL 132(2024)261902

$$m_t^{\text{MC}} = 172.52 \pm 0.14(\text{stat.}) \pm 0.30(\text{syst.})\ \text{GeV} = 172.52 \pm 0.33\ \text{GeV}$$

Extraction of top quark pole mass

Measured σ_{tt} can be used to extract pole mass m_t^{pole}, assuming a value of α_S (or vice versa - assume m_t^{pole} and extract α_S).

σ_{tt} results depend on assumed top mass as kinematics/acceptance depend on m_t.

Precision of ~2 GeV on m_t^{pole} limited by PDF and scale uncertainties on pred[n]

Simultaneous χ^2 fits to 7+8 TeV σ_{tt} provides very precise α_S extraction

PDF set	m_t^{pole} $(\alpha_s = 0.118 \pm 0.001)$	$\alpha_s(m_Z)$ $(m_t = 172.5 \pm 1.0 \text{ GeV})$
CT14	$174.0^{+2.3}_{-2.3}$ GeV	$0.1161^{+0.0030}_{-0.0033}$
MMHT2014	$174.0^{+2.1}_{-2.3}$ GeV	$0.1160^{+0.0031}_{-0.0030}$
NNPDF3.1_a	$173.4^{+1.8}_{-2.0}$ GeV	$0.1170^{+0.0021}_{-0.0018}$

Top pair spin correlations

Production of top-quark pair

Top quark = ideal candidate for spin measurements:

$$\frac{1}{m_t} < \frac{1}{\Gamma_t} < \frac{1}{\Lambda_{QCD}} < \frac{m_t}{\Lambda^2}$$

production 10^{-27} s | lifetime 10^{-25} s | hadronization 10^{-24} s | spin$-$flip 10^{-21} s

- ✓ very short lifetime allows measuring polarization of tops and spin correlation in $t\bar{t}$ production
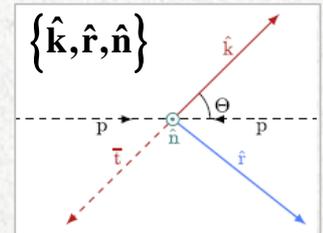- ✓ spin information preserved in the angular distribution of its decay products
- ✓ Gluon emission unlike to do $\Delta S \neq 0$
- ✓ Considered parton reactions: $gg, q\bar{q} \rightarrow t\bar{t} + X \rightarrow b\bar{b} + 4f + X$, $f = q, l, \nu$

Spin state of $t\bar{t}$ system: Hilbert space $\mathcal{H} = \mathcal{H}_t \otimes \mathcal{H}_{\bar{t}}$ with base: $\left\{ |\uparrow\uparrow\rangle, |\uparrow\downarrow\rangle, |\downarrow\uparrow\rangle, |\downarrow\downarrow\rangle \right\}$
(where $|\uparrow\uparrow\rangle \equiv |\uparrow\rangle \otimes |\uparrow\rangle ...$) is described by density matrix:

$$\rho = \tfrac{1}{4}\left[I_4 + \sum_i \left(B_i^+ \sigma^i \otimes I_2 + B_i^- I_2 \otimes \sigma^i \right) + \sum_{i,j} C_{ij} \sigma^i \otimes \sigma^j \right] \quad (10)$$

$\{\hat{k}, \hat{r}, \hat{n}\}$

- With $i, j = 1, 2, 3$, $I_n \equiv n \times n$ identity matrix, $I_4 = I_2 \otimes I_2$, $\sigma^i \equiv$ Pauli matrices
- 2nd term: individual polarization of t and anti-t quarks, ($B_i^+ = \langle \sigma^i \otimes I_2 \rangle$ and $B_i^- = \langle I_2 \otimes \sigma^i \rangle$).
- 3rd term: spin correlation between t and $\bar{t}$, encoded by spin corr. matrix C_{ij} ($= \langle \sigma^i \otimes \sigma^j \rangle$)

Spin quantum state of a top-quark pair (2 qubit system) is determined in general by 15 parameters, $B^{\pm}_i, C_{ij}$

The square of the matrix element for $t\bar{t}$ production and decay to two leptons:

$$\left| M\left(q\bar{q}/gg \to t\bar{t} \to \ell^+ \nu b\, \ell^- \bar{\nu}\bar{b} \right) \right|^2 \propto \Gamma_{ab} R_{ab,\bar{a}\bar{b}} \bar{\Gamma}_{\bar{a}\bar{b}}$$

(11)

$R \equiv$ the production spin density matrix related to on-shell $t\bar{t}$ production, and
Γ and $\bar{\Gamma} \equiv$ the decay spin density matrices for the top and anti-top,
$a, b, \bar{a}, \bar{b} \equiv$ spin indexes of top, anti-top quark spin indexes

The aim of analysis: to study the properties of the R matrix - it is purely a function of the partonic initial state and production dynamics with corresp. kinematic variables.

The production spin density matrix $\mathbf{R}$ can be decomposed in the t and $\bar{t}$ spin spaces using a Pauli matrix basis[1]:

$$\mathbf{R} \propto \tilde{A}\,\mathbf{I}_2 \otimes \mathbf{I}_2 + \sum_i \left(\tilde{B}_i^+ \sigma^i \otimes \mathbf{I}_2 + \tilde{B}_i^- \mathbf{I}_2 \otimes \sigma^i \right) + \sum_{i,j} \tilde{C}_{ij} \sigma^i \otimes \sigma^j$$

(12)

- $\tilde{A} \equiv$ diff. $t\bar{t}$ production cross section (top-quark kinematic distributions)
- $\tilde{B} \equiv$ 3-dim vectors of functions that characterize the degree of t and $\bar{t}$ polarization in each direction in the zero-momentum frame (ZMF).
- $\tilde{C} \equiv$ 3×3 matrix of functions that characterize correlations between t and $\bar{t}$ spins.

The proper spin density matrix $\rho\left(M_{t\bar{t}}, \hat{k} \right)$ and actual $B_i^\pm$ and C_{ij} of $t\bar{t}$ pair:

$$\rho = R/\mathrm{Tr}(R) = R/4\tilde{A}, \quad B_i^\pm = \tilde{B}_i^\pm / \tilde{A}, \quad C_{ij} = \tilde{C}_{ij} / \tilde{A}$$

(13)

The $t\bar{t}$ production is described by the invariant mass $M_{t\bar{t}}$ and top direction $\hat{k}$ in the $t\bar{t}$ center-of-mass (CM) frame.

$$M_{t\bar{t}}^2 = s_{t\bar{t}} = 4\left(m_t^2 + \mathbf{k}^2\right), \quad |\mathbf{k}| = m_t\,\beta\Big/\sqrt{1-\beta^2}\,, \quad \cos\Theta = \hat{k}\cdot\hat{p} \tag{14}$$

$\tilde{A}$ determines the diff. X-sec for $t\bar{t}$ production at fixed $M_{t\bar{t}}^2$ and $\hat{k}$ (top direction):

$$\frac{d\sigma}{d\Omega\,dM_{t\bar{t}}} = \frac{\alpha_S^2\,\beta}{M_{t\bar{t}}^2}\,\tilde{A}\left(M_{t\bar{t}},\hat{k}\right) \tag{15}$$

$\Omega \equiv$ the solid angle associated with $\hat{k}$ and $\alpha_s \approx 0.118$ (strong coupling constant).

The production spin density matrix R is computed via partonic processes R^I :

$$R\left(M_{t\bar{t}},\hat{k}\right) = \sum_{I=q\bar{q},gg} L^I\left(M_{t\bar{t}}\right) R^I\left(M_{t\bar{t}},\hat{k}\right) \tag{16}$$

Each initial state $I = q\bar{q}, gg$ leads to a different $t\bar{t}$ quantum state

$L^I\left(M_{t\bar{t}}\right) \equiv$ luminosity function - incidence of initial partonic state $I = q\bar{q}, gg$.

Top-pair decay products frame

A common coordinate system for *t* and ~~anti-*t*~~ from ~~lab frame~~ → *tt̃ system* is boosted to rest → individual tops are boosted to ~~rest~~. Decay products of the tops are measured in this frame.

The decay spin density matrix is defined as

$$\Gamma_{ab} \equiv M\left(t_a \to \ell\nu_\ell b\right) M\left(t_b \to \ell\nu_\ell b\right)^* \quad \Rightarrow \quad \tilde{\Gamma}_{ab}\left(\hat{\Omega}\right) \propto \delta_{ab} + \kappa\hat{\Omega}_i\sigma^i \qquad (17)$$

Integrating out most of the decay phase space, leaving over only the unit vector $\hat{\Omega}$ of one particle (ℓ) in the top rest frame: $\Gamma \to \tilde{\Gamma}\left(\hat{\Omega}\right)$ - it can be expanded in Pauli matrices

$a, b \equiv$ top quark spin indexes, $\kappa \equiv$ analyzing power (SM: $\kappa_{\ell/d} = +1, \kappa_{\nu/u} = -0.3, \kappa_b = +0.3$),

$\hat{\Omega} = \left(\cos\theta\cos\phi, \cos\theta\sin\phi, \cos\theta\right) \equiv$ particle's unit vector,

$\theta \equiv$ polar angle (with respect z-axis) $\phi \equiv$ azimuthal angle.

One decay particle from each side + contracting through the spin indices
$\Rightarrow$ the spin structure of production matrix elements :

$$\frac{d\sigma}{d\Omega d\bar{\Omega}} \propto \left(\delta_{ab} + \kappa\hat{\Omega}_i\sigma^i_{ab}\right)\tfrac{1}{4}A\left(\delta_{ab}\delta_{\bar{a}\bar{b}} + P^j\sigma^j_{ab}\delta_{\bar{a}\bar{b}} + \bar{P}^{\bar{j}}\delta_{ab}\sigma^{\bar{j}}_{\bar{a}\bar{b}} + C^{k\bar{k}}\sigma^k_{ab}\sigma^{\bar{k}}_{\bar{a}\bar{b}}\right)\left(\delta_{\bar{a}\bar{b}} + \bar{\kappa}\hat{\bar{\Omega}}_{\bar{i}}\sigma^{\bar{i}}_{\bar{a}\bar{b}}\right) =$$

$$= A\left(1 + \kappa\hat{\Omega}_i P^i + \bar{\kappa}\hat{\bar{\Omega}}_{\bar{i}}\bar{P}^{\bar{i}} + \kappa\bar{\kappa}\hat{\Omega}_i C^{i\bar{i}}\hat{\bar{\Omega}}_{\bar{i}}\right), \quad \text{using } \mathrm{Tr}\left(\sigma^i\right) = 0, \quad \sigma^i_{ab}\sigma^j_{ab} = 2\delta^{ij} \qquad (18)$$

Assuming di-lepton channel: $\hat{\Omega} = \hat{\ell}^+, \hat{\bar{\Omega}} = \hat{\ell}^-, \vec{P} = \vec{B}^+, \vec{\bar{P}} = \vec{B}^-, \kappa = 1, \bar{\kappa} = -1$

Spin correlation

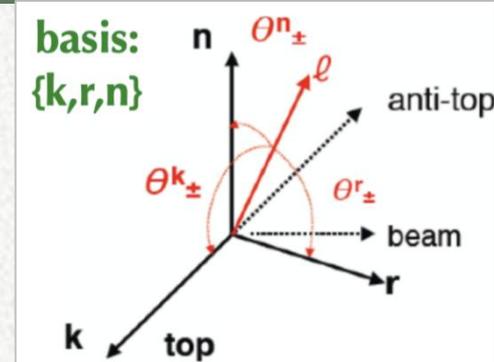Angular distribution of top decay products in helicity basis:

$$\frac{1}{\sigma}\frac{d\sigma}{d\Omega_+ d\Omega_-} = \frac{1}{(4\pi)^2}\left(1 + \vec{B}^+ \cdot \hat{\ell}^+ + \vec{B}^- \cdot \hat{\ell}^- - \hat{\ell}^+ \cdot C \cdot \hat{\ell}^-\right) \quad (19)$$

polarization   spin correlation

$\vec{B}^\pm \equiv$ top/antitop spin polarization vectors (6 components)

$C \equiv$ spin correlation matrix (9 components).

$\hat{\ell}^\pm \equiv$ unit vector in lepton momentum direction

basis: n

{k,r,n}   anti-top

beam

k   top

helicity basis used: {**k, r, n**}

For each of the 15 coefficients (making up $B^\pm$ and C) a variable can be made to obtain a single diff. X-section that depends only on that coefficient.
After integrating out the azimuthal angles:

$$\frac{1}{\sigma}\frac{d\sigma}{d\cos\theta_+^i d\cos\theta_-^j} = \tfrac{1}{4}\left(1 + B_i^+ \cos\theta_+^i + B_i^- \cos\theta_-^i + C_{ij}\cos\theta_+^i \cos\theta_-^j\right) \qquad (20)$$

Leptons' angles in $\left\{\hat{\mathbf{k}},\hat{\mathbf{r}},\hat{\mathbf{n}}\right\}$: $\theta_\pm^k = \sphericalangle\left(\hat{\mathbf{k}},\ell^\pm\right), \theta_\pm^r = \sphericalangle\left(\hat{\mathbf{r}},\ell^\pm\right), \theta_\pm^n = \sphericalangle\left(\hat{\mathbf{n}},\ell^\pm\right)$

By integrating out one of the angles, we can derive single-diff. X-sect. with respect to $\cos\theta_+^i, \cos\theta_-^i$ and $\cos\theta_+^i \cos\theta_-^i$:

$$\frac{1}{\sigma}\frac{d\sigma}{d\cos\theta_+^i} = \tfrac{1}{2}\left(1 + B_i^+ \cos\theta_+^i\right), \qquad \frac{1}{\sigma}\frac{d\sigma}{d\cos\theta_-^i} = \tfrac{1}{2}\left(1 + B_i^- \cos\theta_-^i\right)$$

$$\frac{1}{\sigma}\frac{d\sigma}{dx} = \tfrac{1}{2}\left(1 - C_{ij}x\ln\left(\frac{1}{|x|}\right)\right), \quad x = \cos\theta_+^i \cos\theta_-^i \qquad (21)$$

Similarly for other correlation coef's $\longrightarrow$

To determine the **15 coef.'s**, the $t\bar{t}$ production Xsec can be measured as a function of each of the following 15 observables at the parton level:

✓ $3\cos\theta_1^i + 3\cos\theta_2^i \quad \rightarrow$ to measure $\boldsymbol{B_1^i}$ and $\boldsymbol{B_2^i}$, the top quark and antiquark polarization coef's with respect to each reference axis i.

✓ The $3\cos\theta_1^i\cos\theta_2^i$ terms to measure C_{ii}, the diagonal spin correlation coef. for each axis i.

✓ The $6\ \cos\theta_1^i\cos\theta_2^j \pm \cos\theta_1^j\cos\theta_2^i$ sum and difference terms to measure $C_{ij} \pm C_{ji}$ of the cross spin correlation coef.'s for each $i \neq j$.

Observable	Coefficient	Coefficient function
$\cos\theta_1^k$	B_1^k	b_k^+
$\cos\theta_2^k$	B_2^k	b_k^-
$\cos\theta_1^r$	B_1^r	b_r^+
$\cos\theta_2^r$	B_2^r	b_r^-
$\cos\theta_1^n$	B_1^n	b_n^+
$\cos\theta_2^n$	B_2^n	b_n^-
$\cos\theta_1^k\cos\theta_2^k$	C_{kk}	c_{kk}
$\cos\theta_1^r\cos\theta_2^r$	C_{rr}	c_{rr}
$\cos\theta_1^n\cos\theta_2^n$	C_{nn}	c_{nn}
$\cos\theta_1^r\cos\theta_2^k + \cos\theta_1^k\cos\theta_2^r$	$C_{rk} + C_{kr}$	c_{rk}
$\cos\theta_1^r\cos\theta_2^k - \cos\theta_1^k\cos\theta_2^r$	$C_{rk} - C_{kr}$	c_n
$\cos\theta_1^n\cos\theta_2^r + \cos\theta_1^r\cos\theta_2^n$	$C_{nr} + C_{rn}$	c_{nr}
$\cos\theta_1^n\cos\theta_2^r - \cos\theta_1^r\cos\theta_2^n$	$C_{nr} - C_{rn}$	c_k
$\cos\theta_1^n\cos\theta_2^k + \cos\theta_1^k\cos\theta_2^n$	$C_{nk} + C_{kn}$	c_{kn}
$\cos\theta_1^n\cos\theta_2^k - \cos\theta_1^k\cos\theta_2^n$	$C_{nk} - C_{kn}$	$-c_r$
$\cos\varphi$	D	$-(c_{kk}+c_{rr}+c_{nn})/3$
$\cos\varphi_{\text{lab}}$	$A_{\cos\varphi}^{\text{lab}}$	—
$|\Delta\phi_{\ell\ell}|$	$A_{|\Delta\phi_{\ell\ell}|}$	—
$|\Delta\eta_{\ell\ell}|$	$|\Delta\eta_{\ell\ell}|$	—

$$\theta_+^k \equiv \theta_1^k,\ \theta_-^k \equiv \theta_2^k \qquad \frac{1}{\sigma}\frac{d\sigma}{dx} = \tfrac{1}{2}\left(1 + Coef \cdot x \cdot f(x,s)\right)$$

The spin correlation coefficient D:

$$\frac{1}{\sigma}\frac{d\sigma}{d\cos\varphi} = \tfrac{1}{2}\left(1 - D\cos\varphi\right), \quad D = -\tfrac{1}{3}Tr[C] = -\tfrac{1}{3}\left(C_{kk} + C_{rr} + C_{nn}\right) \quad \boldsymbol{\cos\varphi = \hat{\ell}^+ \cdot \hat{\ell}^-} \qquad (22)$$

Two laboratory-frame distributions – the observables:

✓ $\boldsymbol{\cos\varphi_{\text{lab}} = \hat{\ell}_{\text{lab}}^+ \cdot \hat{\ell}_{\text{lab}}^-}$ analog of φ but in lab-system.

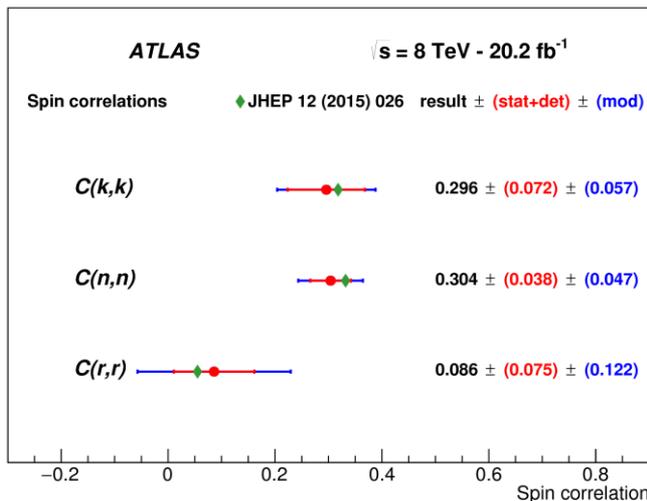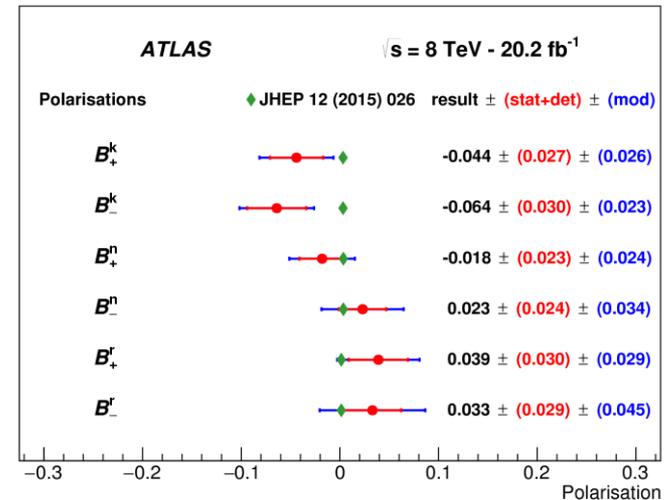✓ $\left|\Delta\varphi_{\ell\ell}\right|$, absolute value of the azimuthal angle difference between the 2ℓ in L-frame.

- Full **spin density matrix** measured at 8 TeV:
- All 3 dilepton channels
- Neutrino-weighting kinem. reconstruction
- Helicity basis $\{\hat{\mathbf{k}}, \hat{\mathbf{r}}, \hat{\mathbf{n}}\}$ is used
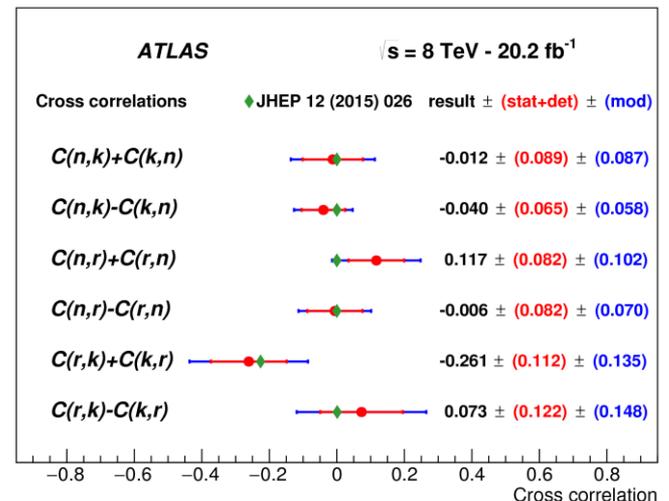- Various unfolded $\cos\Theta^a_\pm$ distributions used to obtain the correlation coefficients:

$$B^a_\pm = 3\langle\cos\theta^a_\pm\rangle, \quad C(a,b) = -9\langle\cos\theta^a_+ \cos\theta^b_-\rangle \quad (23)$$

$$\theta^k_\pm = \sphericalangle(\hat{\mathbf{k}}, \ell^\pm), \theta^r_\pm = \sphericalangle(\hat{\mathbf{r}}, \ell^\pm), \theta^n_\pm = \sphericalangle(\hat{\mathbf{n}}, \ell^\pm)$$

- Results provided for both parton/particle level

$\Diamond \equiv$ SM

JHEP 03(2017)113

ATLAS √s = 8 TeV - 20.2 fb⁻¹

Polarisations — JHEP 12 (2015) 026 result ± (stat+det) ± (mod)

B^k_+	$-0.044 \pm (0.027) \pm (0.026)$
B^k_-	$-0.064 \pm (0.030) \pm (0.023)$
B^n_+	$-0.018 \pm (0.023) \pm (0.024)$
B^n_-	$0.023 \pm (0.024) \pm (0.034)$
B^r_+	$0.039 \pm (0.030) \pm (0.029)$
B^r_-	$0.033 \pm (0.029) \pm (0.045)$

ATLAS √s = 8 TeV - 20.2 fb⁻¹

Spin correlations — JHEP 12 (2015) 026 result ± (stat+det) ± (mod)

$C(k,k)$	$0.296 \pm (0.072) \pm (0.057)$
$C(n,n)$	$0.304 \pm (0.038) \pm (0.047)$
$C(r,r)$	$0.086 \pm (0.075) \pm (0.122)$

ATLAS √s = 8 TeV - 20.2 fb⁻¹

Cross correlations — JHEP 12 (2015) 026 result ± (stat+det) ± (mod)

$C(n,k)+C(k,n)$	$-0.012 \pm (0.089) \pm (0.087)$
$C(n,k)-C(k,n)$	$-0.040 \pm (0.065) \pm (0.058)$
$C(n,r)+C(r,n)$	$0.117 \pm (0.082) \pm (0.102)$
$C(n,r)-C(r,n)$	$-0.006 \pm (0.082) \pm (0.070)$
$C(r,k)+C(k,r)$	$-0.261 \pm (0.112) \pm (0.135)$
$C(r,k)-C(k,r)$	$0.073 \pm (0.122) \pm (0.148)$

Spin correlations vs quantum entaglement

What is quantum entanglement?

Spin correlation and entanglement

Entanglement criteria

Essence of entanglement: quantum state non-separability

Assumption: top-quark pairs production is treated in $t\bar{t}$ CM system spin axis is in top-quark direction - $\left|\uparrow\right\rangle\left(\left|\downarrow\right\rangle\right) \equiv$ top spin is oriented in (against) direction of motion for t and $\bar{t}$.

Production of top-quark pairs in quantum state $\left|F\right\rangle$ vs $\left|S\right\rangle$, $\left|\;\right\rangle_1 \equiv t, \left|\;\right\rangle_2 \equiv \bar{t}$:

$$\left|F\right\rangle,\left|S\right\rangle \in \mathcal{H} = \mathcal{H}_1 \otimes \mathcal{H}_2, \quad \mathcal{H}_1 \equiv \left\{t:\left|\uparrow\right\rangle_1,\left|\downarrow\right\rangle_1\right\}, \quad \mathcal{H}_2 \equiv \left\{\bar{t}:\left|\uparrow\right\rangle_2,\left|\downarrow\right\rangle_2\right\}, \quad \mathcal{H} \equiv \left\{t\bar{t}:\left|\uparrow\uparrow\right\rangle,\left|\uparrow\downarrow\right\rangle,\left|\downarrow\uparrow\right\rangle,\left|\downarrow\downarrow\right\rangle\right\}$$

$$\left|F\right\rangle = \frac{1}{2}\left(\left|\uparrow\right\rangle_1\left|\uparrow\right\rangle_2 - \left|\uparrow\right\rangle_1\left|\downarrow\right\rangle_2 - \left|\downarrow\right\rangle_1\left|\uparrow\right\rangle_2 + \left|\downarrow\right\rangle_1\left|\downarrow\right\rangle_2\right)$$
$$= \frac{1}{\sqrt{2}}\left(\left|\uparrow\right\rangle_1 - \left|\downarrow\right\rangle_1\right) \otimes \frac{1}{\sqrt{2}}\left(\left|\uparrow\right\rangle_2 - \left|\downarrow\right\rangle_2\right)$$

$\in \mathcal{H}_1 \qquad \in \mathcal{H}_2$

quantum state is separable

$$\left|S\right\rangle = \frac{1}{\sqrt{2}}\left(\left|\uparrow\right\rangle_1\left|\downarrow\right\rangle_2 - \left|\downarrow\right\rangle_1\left|\uparrow\right\rangle_2\right)$$
$$\neq (a\left|\uparrow\right\rangle_1 + b\left|\downarrow\right\rangle_1) \otimes (c\left|\uparrow\right\rangle_2 + d\left|\downarrow\right\rangle_2)$$

(24)

quantum state is not separable
Quantum state entanglement

Four maximally entangled states:

$$\left|\Phi^\pm\right\rangle = \tfrac{1}{\sqrt{2}}\left(\left|\uparrow\uparrow\right\rangle \pm \left|\downarrow\downarrow\right\rangle\right), \quad \left|\Psi^\pm\right\rangle = \tfrac{1}{\sqrt{2}}\left(\left|\uparrow\downarrow\right\rangle \pm \left|\downarrow\uparrow\right\rangle\right)$$

(25)

50% 50%

Pure quantum state is separable (entangled), if quantum state can (cannot) be factorised as a product of pure states of both sub-systems.

✓ Physical quantum state $|\psi\rangle \in \mathcal{H}$ is described in general by a density matrix ρ, a nonnegative operator ($\rho = |\psi\rangle\langle\psi|$) in a Hilbert space $\mathcal{H}$, satisfying $\mathrm{Tr}(\rho) = 1$.

Assumption: $t\bar{t}$ pairs are produced in $|F\rangle$ or $|S\rangle$ state. Hilbert space of $t\bar{t}$ production:

$$\mathcal{H} \equiv \left\{ t\bar{t} : |\uparrow\uparrow\rangle, |\uparrow\downarrow\rangle, |\downarrow\uparrow\rangle, |\downarrow\downarrow\rangle \right\}, \quad |F\rangle, |S\rangle \in \mathcal{H}$$

$$|F\rangle = \tfrac{1}{2}\left(|\uparrow\uparrow\rangle - |\uparrow\downarrow\rangle - |\downarrow\uparrow\rangle + |\downarrow\downarrow\rangle \right) = \sqrt{\tfrac{1}{2}}\left(|\uparrow\rangle - |\downarrow\rangle \right) \otimes \sqrt{\tfrac{1}{2}}\left(|\uparrow\rangle - |\downarrow\rangle \right) \qquad \Rightarrow \text{ separable}$$

$$|S\rangle = \sqrt{\tfrac{1}{2}}\left(|\uparrow\downarrow\rangle - |\downarrow\uparrow\rangle \right) \qquad \text{red (blue) colour} \leftrightarrow \text{top (anti-top) quark} \qquad \Rightarrow \text{ entangled}$$

Production spin density matrices for these two states:

$$\rho_F = |F\rangle\langle F| = \tfrac{1}{4}\left(|\uparrow\uparrow\rangle - |\uparrow\downarrow\rangle - |\downarrow\uparrow\rangle + |\downarrow\downarrow\rangle \right) \otimes \left(\langle\uparrow\uparrow| - \langle\uparrow\downarrow| - \langle\downarrow\uparrow| + \langle\downarrow\downarrow| \right) =$$

$$= \tfrac{1}{4}\left(|\uparrow\uparrow\rangle\langle\uparrow\uparrow| - |\uparrow\uparrow\rangle\langle\uparrow\downarrow| - |\uparrow\uparrow\rangle\langle\downarrow\uparrow| + |\uparrow\uparrow\rangle\langle\downarrow\downarrow| \quad - \quad |\uparrow\downarrow\rangle\langle\uparrow\uparrow| + |\uparrow\downarrow\rangle\langle\uparrow\downarrow| + |\uparrow\downarrow\rangle\langle\downarrow\uparrow| - |\uparrow\downarrow\rangle\langle\downarrow\downarrow|$$

$$-|\downarrow\uparrow\rangle\langle\uparrow\uparrow| + |\downarrow\uparrow\rangle\langle\uparrow\downarrow| + |\downarrow\uparrow\rangle\langle\downarrow\uparrow| - |\downarrow\uparrow\rangle\langle\downarrow\downarrow| \quad + \quad |\downarrow\downarrow\rangle\langle\uparrow\uparrow| - |\downarrow\downarrow\rangle\langle\uparrow\downarrow| - |\downarrow\downarrow\rangle\langle\downarrow\uparrow| + |\downarrow\downarrow\rangle\langle\downarrow\downarrow| \right)$$

(26)

$$\rho_S = |S\rangle\langle S| = \tfrac{1}{2}\left(|\uparrow\downarrow\rangle - |\downarrow\uparrow\rangle \right) \otimes \left(\langle\uparrow\downarrow| - \langle\downarrow\uparrow| \right) = \tfrac{1}{2}\left(|\uparrow\downarrow\rangle\langle\uparrow\downarrow| - |\uparrow\downarrow\rangle\langle\downarrow\uparrow| - |\downarrow\uparrow\rangle\langle\uparrow\downarrow| + |\downarrow\uparrow\rangle\langle\downarrow\uparrow| \right)$$

Let us assume $t\bar{t}$ production in states $|F\rangle$ and $|S\rangle$ but we measure only spin states of top quark $\Rightarrow$ A reduced density matrix of top quark can be introduced for both the states in base $\left\{ |\uparrow\rangle, |\downarrow\rangle \right\}$:

$$\rho_F^t = \mathrm{Tr}_{\bar{t}}\, \rho_F = \langle\uparrow|\rho_F|\uparrow\rangle + \langle\downarrow|\rho_F|\downarrow\rangle = \tfrac{1}{2}\left(|\uparrow\rangle\langle\uparrow| - |\uparrow\rangle\langle\downarrow| - |\downarrow\rangle\langle\uparrow| + |\downarrow\rangle\langle\downarrow| \right)$$

$$\rho_S^t = \mathrm{Tr}_{\bar{t}}\, \rho_S = \langle\uparrow|\rho_S|\uparrow\rangle + \langle\downarrow|\rho_S|\downarrow\rangle = \tfrac{1}{2}\left(|\uparrow\rangle\langle\uparrow| + |\downarrow\rangle\langle\downarrow| \right)$$

$$\rho_F^t = \begin{pmatrix} \tfrac{1}{2} & -\tfrac{1}{2} \\ -\tfrac{1}{2} & \tfrac{1}{2} \end{pmatrix}$$

$$\rho_S^t = \begin{pmatrix} \tfrac{1}{2} & 0 \\ 0 & \tfrac{1}{2} \end{pmatrix}$$

(27)

❑ **Definition of entropy**: $S(\rho) = -\text{Tr}\left(\rho \log_2[\rho]\right) \rightarrow S(\rho) = -\sum_{k=1}^{d} \lambda_k \log_2 \lambda_k$

$\lambda_k \equiv$ eigenvalues of ρ, the eigenvalues are nonnegative and a zero eigenvalue contributes zero to the entropy: $\lim_{x \to 0} x \log x = 0$, $d \equiv$ dim. of Hilbert space. **(28)**

Using the entropy we get another criterion for pure states vs mixed states:

pure state: $S(\rho) = 0$ **mixed state:** $S(\rho) > 0$ **(29)**

Entropy interpretation: missing information (in bits) about state.

$\Rightarrow$ there is no missing information for a pure state.

❑ **Spin-flipped** state. For a pure state of a **single qubit**, the spin flip is defined by:

$$\left|\tilde{\psi}\right\rangle = \sigma_2 \left|\psi^*\right\rangle, \quad \sigma_2 = \begin{pmatrix} 0 & -i \\ i & 0 \end{pmatrix} \text{ or } \tilde{\rho} = \sigma_2 \left|\psi^*\right\rangle\left\langle\psi^*\right|\sigma_2$$ **(30)**

Where $\left|\psi^*\right\rangle$ is the complex conjugate of $\left|\psi\right\rangle$, when expressed in basis $\left\{\left|\uparrow\right\rangle, \left|\downarrow\right\rangle\right\}$. For a spin-½ particle it is the **standard time reversal operation**.

For **two qubits** the spin-flipped state is

$$\tilde{\rho} = (\sigma_2 \otimes \sigma_2)\rho^*(\sigma_2 \otimes \sigma_2), \quad \left\{\left|\uparrow\uparrow\right\rangle, \left|\uparrow\downarrow\right\rangle, \left|\downarrow\uparrow\right\rangle, \left|\downarrow\downarrow\right\rangle\right\}$$ **(31)**

where the complex conjugate is taken in for a pair of spin-½ particles basis.

Entanglement *via* concurrence – pure state of 2 qubits:

$$C(\psi) = |\langle \psi | \tilde{\psi} \rangle| \quad \text{and} \quad \text{entanglement} \quad E(\psi) = \mathcal{E}(C(\psi))$$

Where

$$\mathcal{E}(C) = \tfrac{1}{2}\left(1 + \sqrt{1-C^2}\right)\log_2\left(\tfrac{1}{2}\left(1+\sqrt{1-C^2}\right)\right) - \tfrac{1}{2}\left(1 - \sqrt{1-C^2}\right)\log_2\left(\tfrac{1}{2}\left(1-\sqrt{1-C^2}\right)\right)$$

(32)

$\mathcal{E}(C)$ is monotonically increasing and ranges from 0 to 1 as C goes from 0 to 1.

Example 1: the singlet state $|\psi\rangle = \frac{1}{\sqrt{2}}\left(|\uparrow\downarrow\rangle - |\downarrow\uparrow\rangle\right)$ changes by a spin flip only its sign
$\Rightarrow$ its concurrence $|\langle \psi | \tilde{\psi} \rangle| = 1 \Rightarrow \mathcal{E}(C) = 1 \quad \rightarrow$ **entanglement is maximal**.

Example 2: the state $|\psi\rangle = |\uparrow\downarrow\rangle$ applying spin flip $|\uparrow\downarrow\rangle \rightarrow |\downarrow\uparrow\rangle$ what is an orthogonal state
$\Rightarrow$ concurrence $C(\psi) = |\langle \psi | \tilde{\psi} \rangle| = 0 \Rightarrow \mathcal{E}(C) = 0 \rightarrow$ **entanglement = 0**.

The formula for the **entanglement** of formation of a **mixed state** of 2 qubits:

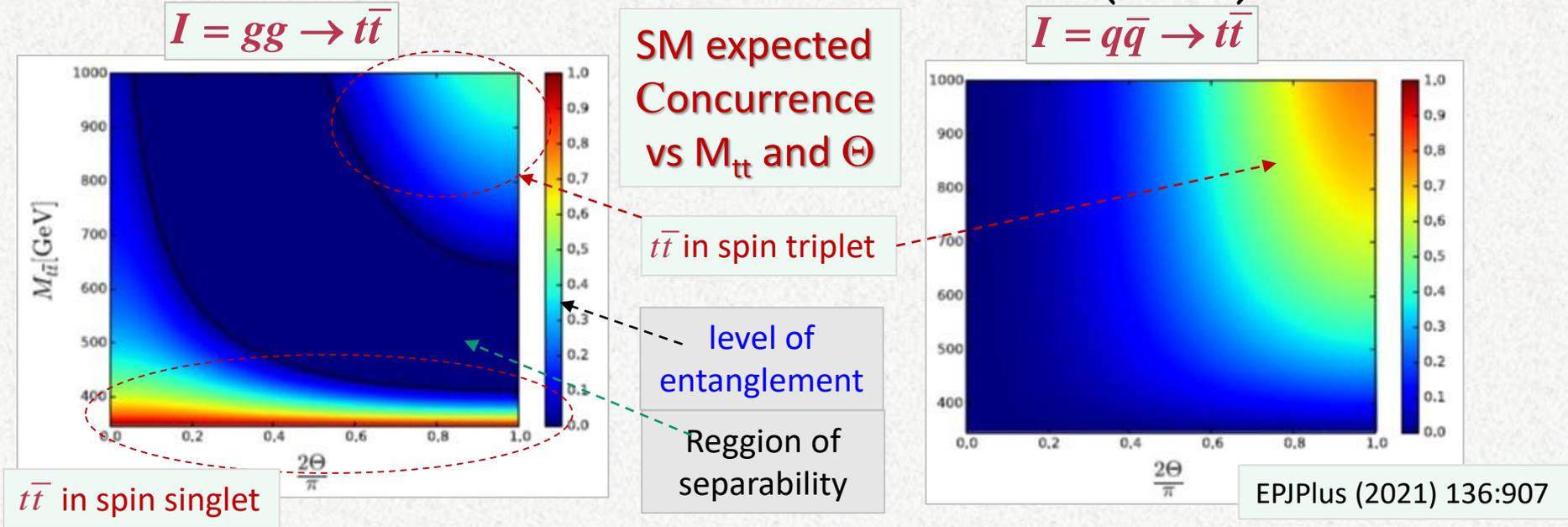$$E(\rho) = \mathcal{E}(C(\rho)), \quad C(\rho) = \max\{0, \lambda_1 - \lambda_2 - \lambda_3 - \lambda_4\}$$

(33)

$\lambda_i \equiv$ eigenvalues, in decreasing order, of Hermitian matrix $R(\rho) = \sqrt{\sqrt{\rho}\,\tilde{\rho}\,\sqrt{\rho}}$

The concurrence satisfies $0 \leq C[\rho] \leq 1$, with a **quantum state being entangled if and only if** $C[\rho] > 0$. States satisfying $C[\rho] = 1$: maximally entangled states.

SM expectations: entanglement as a function of $M_{t\bar{t}}$ and the production angle Θ in the $t\bar{t}$ CM frame - **concurrence** of the spin density matrix $\rho^I\left(M_{t\bar{t}}, \hat{k}\right)$.

$I = gg \to t\bar{t}$

SM expected
Concurrence
vs M_{tt} and Θ

$I = q\bar{q} \to t\bar{t}$

$t\bar{t}$ in spin triplet

level of
entanglement

Reggion of
separability

$t\bar{t}$ in spin singlet

EPJPlus (2021) 136:907

LO: the matrices $\rho^I\left(M_{t\bar{t}}, \hat{k}\right)$ are **unpolarized** and their correlation matrix is **symmetric**. From the Peres–Horodecki criterion:

A. Peres, PRL 77(1996) 1413,
P. Horodecki, PL A232 (1997) 333

the condition $\quad \Delta \equiv -C_{nn} + \left|C_{kk} + C_{rr}\right| - 1 > 0 \quad$ (34)

is a **necessary** and **sufficient condition** for the presence of entanglement, with the concurrence simply given by:

$$C[\rho] = \tfrac{1}{2}\max\left(\Delta, 0\right)$$

(35)

Observation of entanglement, in $t\bar{t}$ events produced at the LHC, using a proton–proton collision dataset with √s = 13 TeV and Lumi of 140 fb⁻¹ recorded with the ATLAS experiment.

- Dilepton $t\bar{t}$ events used in the analysis
- Used observable: cosφ, $\varphi \equiv \sphericalangle\left(\ell^+, \ell^-\right)$
- data divided into 3 regions based on $m_{t\bar{t}}$:
  Signal region: $340 < m_{t\bar{t}} < 380$ GeV
  (near prod. threshold) +2 valid. regions.

Entanglement marker D extracted from

$$\frac{1}{\sigma}\frac{d\sigma}{d\cos\varphi} = \frac{1}{2}\left(1 - D\cos\varphi\right), \quad D = -\frac{1}{3}\left(C_{kk} + C_{rr} + C_{nn}\right)$$

Entanglement marker D *is* calculated from detector-level cos distribution - **entanglement: D < -1/3**

Signal region D marker

Data agree with predictions!

Background: Single top + W boson (tW), $t\bar{t}$ + 1 boson (H, W, Z) and dilepton events from 1 or 2 gauge bosons (W, Z).

Nature 633 (2024) 542

ATLAS
$\sqrt{s}$ = 13 TeV, 140 fb^{-1}

Legend:
- Limit (Powheg + Herwig7)
- Limit (Powheg + Pythia8)
- Theory Uncertainty
- Data
- Powheg + Pythia8 (hvq)
- Powheg + Herwig7 (hvq)

Y-axis: Particle-level D

X-axis categories: $340 < m_{t\bar{t}} < 380$, $380 < m_{t\bar{t}} < 500$, $m_{t\bar{t}} > 500$

Particle-level Invariant Mass Range [GeV]

Nature 633 (2024) 542

SM: Entanglement cond.:
  $D < -1/3$ (parton level)

Entanglement limit for Powheg + Pythia:
-0.322 ± 0.009 $\Rightarrow$

Entanglement observation !
$\gg 5\sigma$ limit below

Measurement of the particle-level D in the validation and signal regions:

$380 < m_{t\bar{t}} < 500$ GeV: $D = -0.265 \pm 0.001\,(\text{stat.}) \pm 0.019\,(\text{syst.})$

$m_{t\bar{t}} > 500$ GeV: $D = -0.093 \pm 0.001\,(\text{stat.}) \pm 0.021\,(\text{syst.})$

Signal region: $D = -0.537 \pm 0.002\,(\text{stat.}) \pm 0.019\,(\text{syst.})$

CMS: Dilepton analysis: strategy

- Focus on low-mass region ($345 < m_{t\bar{t}} < 400$ GeV) to increase entanglement – expected in gg fusion channel.

- Cut on velocity along the beam line of the $t\bar{t}$ system to increase fraction:

$$\beta = \left| \frac{p_z^t + p_z^{\bar{t}}}{E^t + E^{\bar{t}}} \right| < 0.9$$

- Top quark reconstructions with $m_{\ell b}$ weighting method.

- To measure helicity angle $\cos\varphi = \hat{\ell}_1 \cdot \hat{\ell}_2$ - fully encapsulates spin correlations information for gg channel.

- Perform a profile maximum likelihood fit of the $\cos\varphi$ distribution in the $m_{t\bar{t}}$- β signal region.

- $D = -(1+\Delta)/3 < -1/3 \rightarrow$ entangled.

$D = 0$ ($\Delta = 1$) : no spin correlations in $t\tilde{t}$,
$D = -1$ ($\Delta = 0$): maximally entangled $t\tilde{t}$.

MC $t\tilde{t}$ simulation (gg fusion): boundary for entanglement

Focused phase space

$$1 + \Delta = C_{11} + C_{22} + C_{33} = -3D$$

Signal modeling

- Combined signal model: $t\bar{t}$ + toponium (η_t)

- PowhegBox+Pythia8 (NLO) as nominal $t\bar{t}$ sample
  - inclusion of EWK corrections at NLO with HATHOR
  - p_T reweighting to NNLO QCD calculations

- Toponium model generated with MG5 aMC@NLO(LO)+Pythia8   PRD 104 034023
  - only pseudoscalar gg colour singlet and spin-0 state accounted for
  - improves data modeling at threshold

Toponium: predicted top quark-antiquark quasi-bound state with a mass of 343 GeV and a width of 7 GeV.

Result of likelihood fit: the best fit PH+P8+η_t.

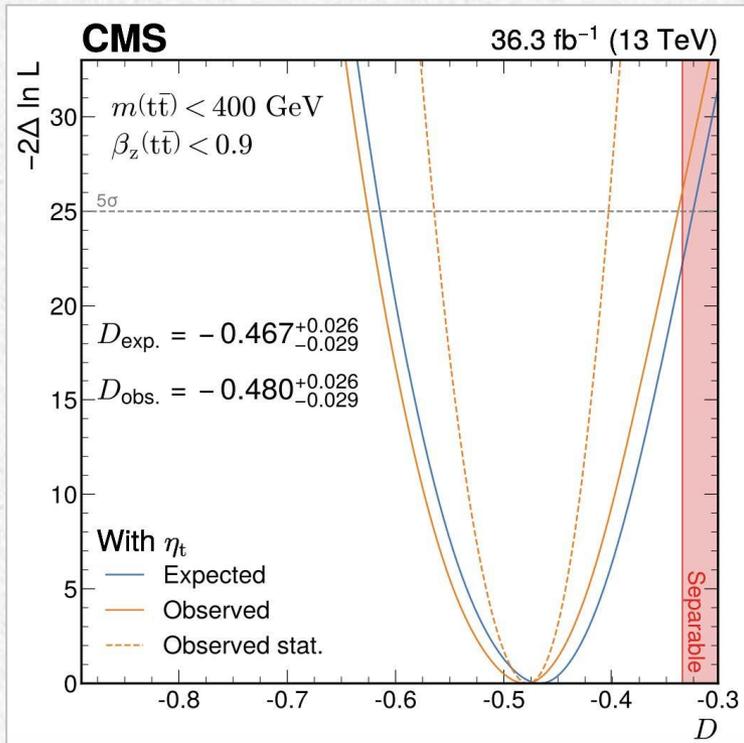JHEP 06(2020) 158

Dilepton analysis region: $345 < m_{t\bar{t}} < 400$ GeV

- Scan of the $-2\Delta \ln L$ distribution yields at parton level, accounting for all detector effects.

$$D_{\mathrm{obs}} = -0.480^{+0.016}_{-0.017}\,(\mathrm{stat})^{+0.020}_{-0.023}\,(\mathrm{syst})$$

$$D_{\mathrm{exp}} = -0.467^{+0.016}_{-0.017}\,(\mathrm{stat})^{+0.021}_{-0.024}\,(\mathrm{syst})$$

- Significance: 5.1 obs (4.7 exp.)

Good agreement with SM predictions !

Forward-backward / charge asymmetry in tt-bar production

The $p\overline{p}$ collisions (Tevatron experiments):

- FB asymmetry: $N(t \to p)$ t in p direction vs $N(t \to \overline{p})$: t in $\overline{p}$ direction
- Charge asymmetry: $N(t \to p)$ vs $N(\overline{t} \to p)$

At pp collisions (LHC experiments) only charge asymmetry!

SM: LO strong interaction processes $q + \overline{q} \to Q + \overline{Q}$ and $g + g \to Q + \overline{Q}$: no A_{FB}!

A_{FB}: interference of amplitudes with the same initial/final state particles.

Gluon fusion is symmetric in all orders asymmetry arise due to quark annihilation!
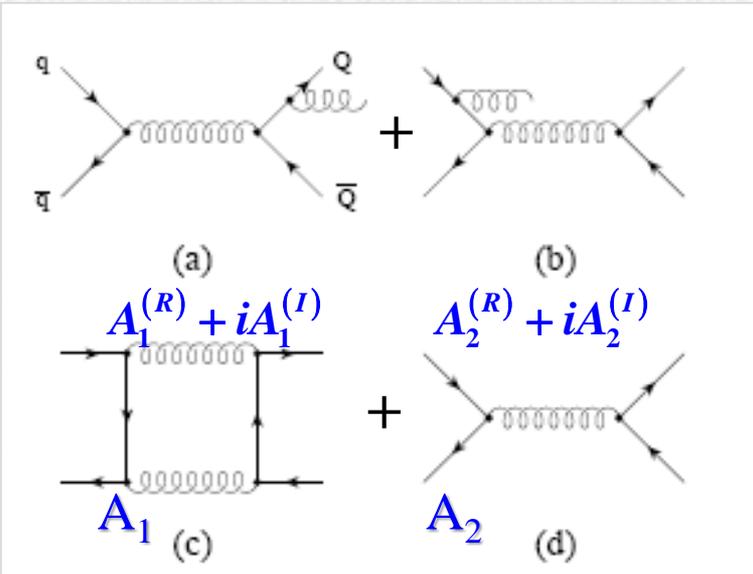

(a)   (b)

(c)   (d)

(a)   (b)

(c)   (d)   (e)

✓ Interference of final-state (a) with initial-state (b) gluon radiation amplitude

✓ Interference of the box (c) with Born diagram (d)

Charge asymmetry through flavor excitation in quark-gluon interaction (small contribution)

The dependence of the SM asymmetry on QCD radiation is strong:

Negative asymmetry

$A_1^{(R)} + iA_1^{(I)}$ $A_2^{(R)} + iA_2^{(I)}$

A_1 A_2

⟶ Negative asymmetry
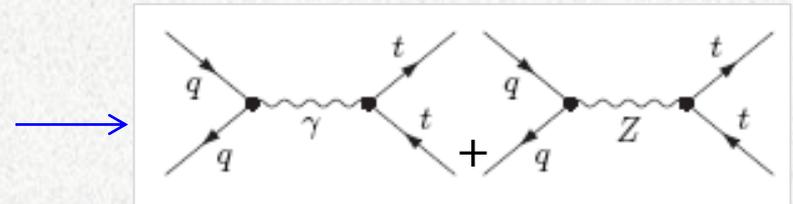
Contribution ~ α_s^3

In reality both are infinite and cannot be treated independently

⟶ Positive asymmetry

asymmetry

$$\text{Cross section} \sim |A|^2 \Rightarrow |A|^2 = \left(A_1 + A_2\right)\left(A_1^* + A_2^*\right) = |A_1|^2 + |A_2|^2 + \underbrace{A_1 A_2^* + A_1^* A_2}_{} \quad (1)$$

Non negligible contribution from to $t\bar{t}$ A_{FB} (A_{Ch}) comes from **EW processes** (~20% of QCD, Hollik and Pagani, arXiv.1107.2606):
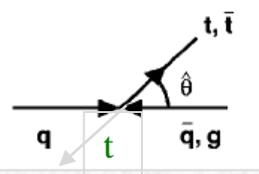
- Purely electroweak processes ⟶

- QED − QCD interference at $O\left(\alpha_S^2 \alpha\right)$: from $q\bar{q} \to t\bar{t}$, $q\bar{q} \to t\bar{t}g$, $q\bar{q} \to t\bar{t}\gamma$

SM: A_{FB}/A_C formulae, $q\bar{q}$ rest frame

At partonic level: charge asymmetry   forward-backward asymmetry

$$\hat{A}_{Ch}\left(\cos\hat{\theta}\right) = \frac{N_Q(\cos\hat{\theta}) - N_{\bar{Q}}(\cos\hat{\theta})}{N_Q(\cos\hat{\theta}) + N_{\bar{Q}}(\cos\hat{\theta})}$$

$$\hat{A}_{FB}\left(\cos\hat{\theta}\right) = \frac{N_Q(\cos\hat{\theta}) - N_Q(-\cos\hat{\theta})}{N_Q(\cos\hat{\theta}) + N_Q(-\cos\hat{\theta})} \quad (3)$$
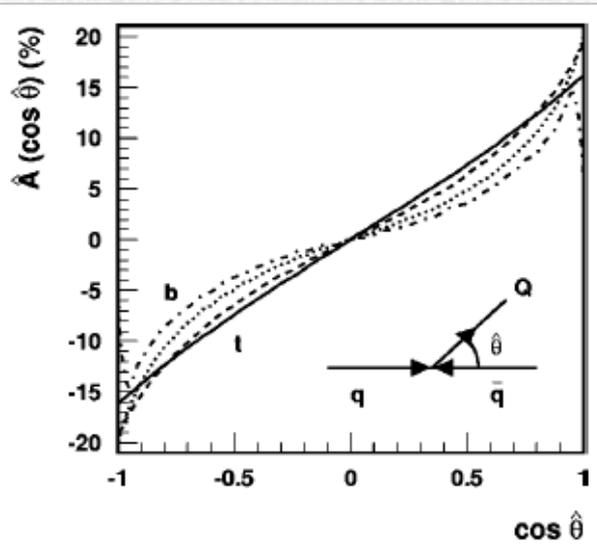
$\hat{\theta} \equiv$ $Q (=t,b)$ production angle in $q\bar{q}$ rest frame, $N\left(\cos\hat{\theta}\right) = \frac{d\sigma}{d\Omega}\left(\cos\hat{\theta}\right)$

Assuming CP conservation:

$$N_{\bar{Q}}(\cos\hat{\theta}) = N_Q(-\cos\hat{\theta}) \Rightarrow \hat{A}_{Ch} = \hat{A}_{FB} \quad (4)$$

Integrated charge/FB asymmetry:

$$\bar{\hat{A}} = \frac{N_Q(\cos\hat{\theta} \geq 0) - N_{\bar{Q}}(\cos\hat{\theta} \geq 0)}{N_Q(\cos\hat{\theta} \geq 0) + N_{\bar{Q}}(\cos\hat{\theta} \geq 0)} \quad (5)$$
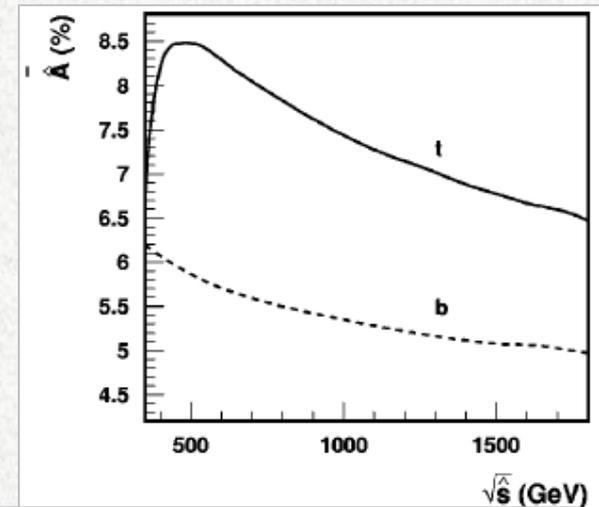
SM prediction for $t\bar{t}$ A_{FB} ($q\bar{q}$ rest frame):

$p\bar{p}$ collisions, 1.96 TeV

✓Integrated $A_{FB} \approx$ 6-8.5%

✓Differential A_{FB}: maximum at $\cos\theta = \pm1$

Kuhn et al., PRD59 054017(1999)

Top quarks preferentially emitted in quark direction

Using rapidity instead of $\boldsymbol{cos\theta}$ for A_{FB} (diff. and integrated) in $p\bar{p}$ rest frame one gets:

$$y = \frac{1}{2}\ln\frac{E+p_L}{E-p_L} \quad\Rightarrow\quad A_{FB}^{p\bar{p}}(y_t) = \frac{N(y_t)-N(-y_t)}{N(y_t)+N(-y_t)} \qquad A_{FB}^{p\bar{p}} = \frac{N(y_t>0)-N(y_t<0)}{N(y_t>0)+N(y_t<0)} \qquad (6)$$

Charge asymmetry is got by: $N(-y_t)\rightarrow N(y_{\bar{t}})$ (CP conservation: $N(-y_t)=N(y_{\bar{t}})$)

Assuming CP the A_{FB} can be expressed through variable $\varDelta y_t = y_t - y_{\bar{t}}$ (is invariant under a boost along beam - the same in both $p\bar{p}$ and $t\bar{t}$ rest frame.

The t-quark production angle, θ, in $t\bar{t}$ rest frame vs. $\varDelta y_t$:

$$\varDelta y_t = 2\tanh^{-1}(\beta\cos\theta), \quad \beta = \sqrt{1-4m_{top}^2/\hat{s}} \qquad (7)$$

The asymmetry (integrated and differential):

$$A_{FB}^{t\bar{t}} = \frac{N(\varDelta y_t>0)-N(\varDelta y_t<0)}{N(\varDelta y_t>0)+N(\varDelta y_t<0)}, \quad A_{FB}^{t\bar{t}}(\varDelta y_t) = \frac{N(\varDelta y_t)-N(-\varDelta y_t)}{N(\varDelta y_t)+N(-\varDelta y_t)} \qquad (8)$$
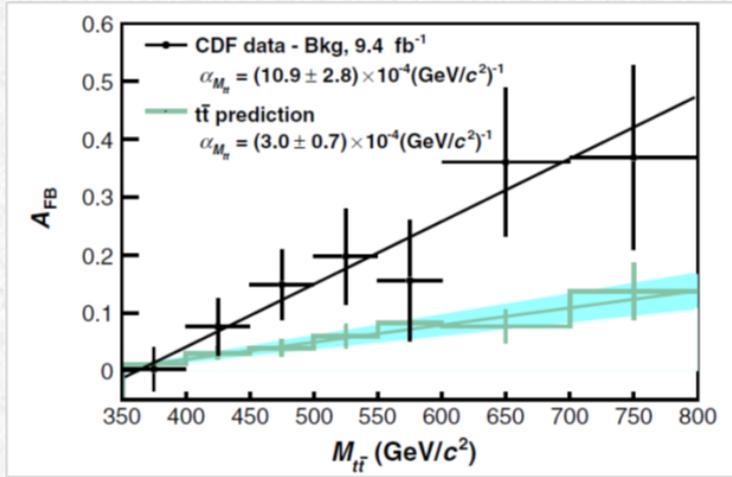
Theory: Inclusive parton-level asymmetries in $t\bar{t}$ frames

NNLO[1]: $A_{FB}^{t\bar{t}} = \boldsymbol{0.095 \pm 0.007}$ and aN³LO (gluon resumm.)[2]: $A_{FB}^{t\bar{t}} = \boldsymbol{0.100 \pm 0.006}$

|[1]≡ Phys. Rev. Lett. 115,052001 (2015) |[2]≡ Phys. Rev. D 91, 071502 (2015).

CDF and D0 differential A_{FB} reconstructed in **ℓ+jets** channels as a function of $m_{t\bar{t}}$ vs SM

CDF, L=9.4fb⁻¹

ℓ+ jets , 2ℓ

$A^{t\bar{t}}_{\text{FB}} = 0.164 \pm 0.047$ $A^{t\bar{t}}_{\text{FB}} = 0.12 \pm 0.11 \pm 0.07$

D0, L=9.7fb⁻¹

ℓ+ jets , 2ℓ

$A^{t\bar{t}}_{\text{FB}} = 0.106 \pm 0.030$ $A^{t\bar{t}}_{\text{FB}} = 0.175 \pm 0.063$

Tevatron $t\bar{t}$ asymmetry summary

LHC/ATLAS: Charge Asymmetry

- LHC: $t\bar{t}$ produced mainly in $gg \to t\bar{t}$ events and an asymmetry can be seen only in $q\bar{q} \to t\bar{t}$ and $qg \to t\bar{t}q \Rightarrow A_C$ is strongly diluted!

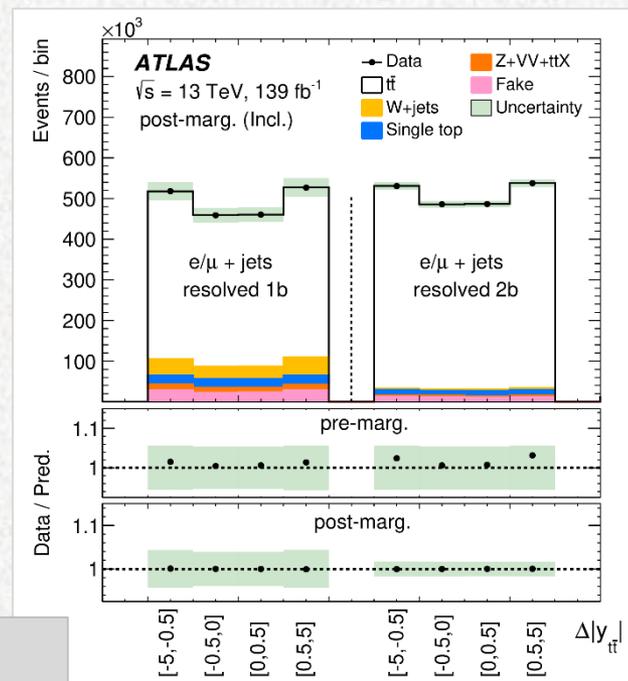- Charge asymmetry for $t\bar{t}$ production:

$$A_C = \frac{N(\Delta|y| > 0) - N(\Delta|y| < 0)}{N(\Delta|y > 0|) + N(\Delta|y| < 0)}, \quad \text{where} \quad \Delta|y| = |y_t| - |y_{\bar{t}}| \qquad (9)$$

- Top quarks preferentially emitted in quark direction: proton's quarks generally carry a larger momentum fraction than antiquarks (sea quarks), tops tends to be more forward than anti-tops in the lab frame.

- SM: charge asymmetry is calculated at NNLO accuracy in the strong coupling and with NLO EW corrections predicts to be

$$A_C^{\text{theo}} = \mathbf{0.0064}\,{}^{+0.0005}_{-0.0006} \qquad \text{(Czakon et al., PRD 98(2018)014603)}$$

uncertainty: variation of μ_R and μ_F scales +PDF uncert.

Contribution of EW interaction is $(5 - 10 \times \text{lower})$

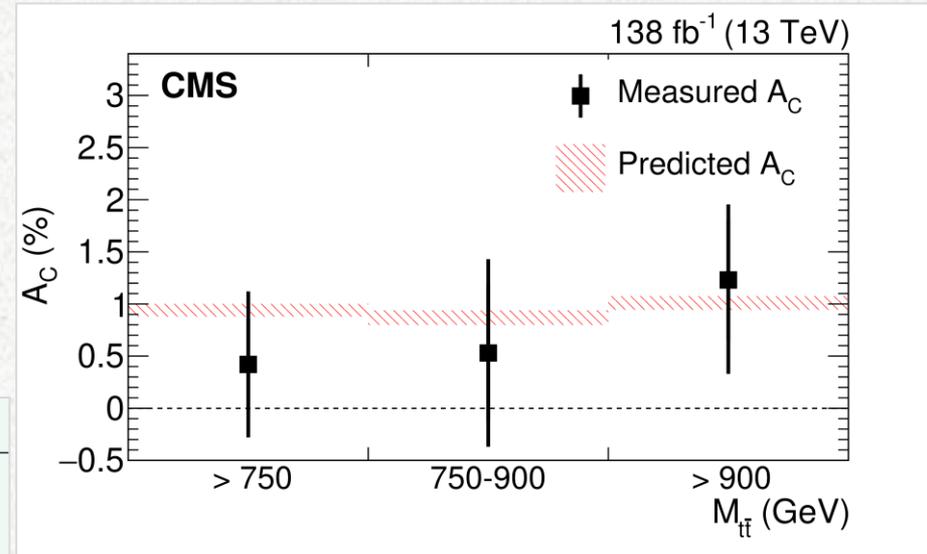Comparison data vs prediction for reconstructed $\Delta|y_{t\bar{t}}|$ in inclusive $A_C^{t\bar{t}}$

✓ Charge asymmetry in top quark pairs using ℓ+jets topology ($\ell=\mu$ or e)

✓ pp collisions at √s= 13 TeV, an integrated luminosity of 138 fb⁻¹.

✓ Selection: optimized for top quarks produced with large Lorentz boosted (non-isolated leptons and overlapping jets) + $t\bar{t}$ invariant mass $\geq$ 750 GeV

✓ unfolded distributions for e and μ channels: using a binned maximum likelihood fit.

The measured top quark charge asymmetry

$$A_C = \left(0.42^{+0.64}_{-0.69}\right)\% , \quad A_C^{\text{theo}} = \left(0.94^{+0.05}_{-0.07}\right)\%$$

The predicted and measured results for also two invariant mass ranges,

- 750-900 and >900 GeV
- μ+jets and e+jets channels combined

$M_{t\bar{t}}$ (GeV)	A_C	Stat	Syst	MC stat	Total	Prediction
>750	0.42	±0.44	$^{+0.33}_{-0.44}$	± 0.32	$^{+0.64}_{-0.69}$	0.94 $^{+0.05}_{-0.07}$
750–900	0.53	±0.65	$^{+0.37}_{-0.49}$	± 0.45	$^{+0.87}_{-0.93}$	0.87 $^{+0.06}_{-0.08}$
>900	1.23	±0.58	$^{+0.43}_{-0.84}$	± 0.41	$^{+0.82}_{-1.10}$	1.01 $^{+0.06}_{-0.07}$

Main systematics: μ_R and μ_F, JEC, FSR, PDF, top quark p_T, W+jets, t-tag

Good agreement with the SM prediction at NNLO in QCD + NLO in EW corrections.

Thank you!

Quantum entaglement: present distance records

Non-local correlation between entangled subsystems:

Atoms: Δl = 33 km, Δt = 0.0001 sec

van Leent et al., Nature 607 (2022) 69

$$\Delta l = 10 \text{ m}$$
$$\Delta t \approx 0.00000003 \text{ s}$$

Photons: Δl = **1200 km**, Δt = 0.004 s

Yin et al., Science 356 (2017) 1140

Chinese satellite Micius:

quantum communication

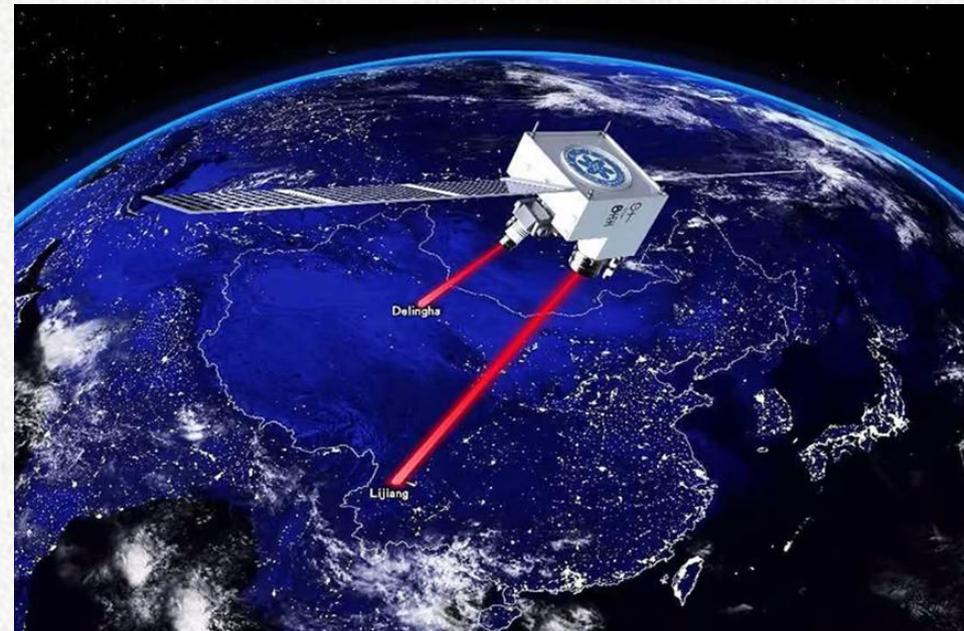| Parameter	Input value	Free in fit	Fit Result	Fit w/o exp. input in line	Fit w/o exp. input in line, no theo. unc.
M_H [GeV]	125.1 ± 0.2	yes	125.1 ± 0.2	90^{+21}_{-18}	89^{+20}_{-17}
M_W [GeV]	80.379 ± 0.013	–	80.359 ± 0.006	80.354 ± 0.007	80.354 ± 0.005
Γ_W [GeV]	2.085 ± 0.042	–	2.091 ± 0.001	2.091 ± 0.001	2.091 ± 0.001
M_Z [GeV]	91.1875 ± 0.0021	yes	91.1882 ± 0.0020	91.2013 ± 0.0095	91.2017 ± 0.0089
Γ_Z [GeV]	2.4952 ± 0.0023	–	2.4947 ± 0.0014	2.4941 ± 0.0016	2.4940 ± 0.0016
σ^0_{had} [nb]	41.540 ± 0.037	–	41.484 ± 0.015	41.475 ± 0.016	41.475 ± 0.015
R^0_ℓ	20.767 ± 0.025	–	20.742 ± 0.017	20.721 ± 0.026	20.719 ± 0.025
$A^{0,\ell}_{FB}$	0.0171 ± 0.0010	–	0.01620 ± 0.0001	0.01619 ± 0.0001	0.01619 ± 0.0001
A_ℓ (⋆)	0.1499 ± 0.0018	–	0.1470 ± 0.0005	0.1470 ± 0.0005	0.1469 ± 0.0003
$\sin^2\theta^\ell_{eff}(Q_{FB})$	0.2324 ± 0.0012	–	0.23153 ± 0.00006	0.23153 ± 0.00006	0.23153 ± 0.00004
$\sin^2\theta^\ell_{eff}$(Tevt.)	0.23148 ± 0.00033	–	0.23153 ± 0.00006	0.23153 ± 0.00006	0.23153 ± 0.00004
A_c	0.670 ± 0.027	–	0.6679 ± 0.00021	0.6679 ± 0.00021	0.6679 ± 0.00014
A_b	0.923 ± 0.020	–	0.93475 ± 0.00004	0.93475 ± 0.00004	0.93475 ± 0.00002
$A^{0,c}_{FB}$	0.0707 ± 0.0035	–	0.0736 ± 0.0003	0.0736 ± 0.0003	0.0736 ± 0.0002
$A^{0,b}_{FB}$	0.0992 ± 0.0016	–	0.1030 ± 0.0003	0.1032 ± 0.0003	0.1031 ± 0.0002
R^0_c	0.1721 ± 0.0030	–	0.17224 ± 0.00008	0.17224 ± 0.00008	0.17224 ± 0.00006
R^0_b	0.21629 ± 0.00066	–	0.21582 ± 0.00011	0.21581 ± 0.00011	0.21581 ± 0.00004
$\overline{m}_c$ [GeV]	$1.27^{+0.07}_{-0.11}$	yes	$1.27^{+0.07}_{-0.11}$	–	–
$\overline{m}_b$ [GeV]	$4.20^{+0.17}_{-0.07}$	yes	$4.20^{+0.17}_{-0.07}$	–	–
m_t [GeV]$^{(\triangledown)}$	172.47 ± 0.68	yes	172.83 ± 0.65	176.4 ± 2.1	176.4 ± 2.0
$\Delta\alpha^{(5)}_{had}(M^2_Z)$ $^{(\dagger\triangle)}$	2760 ± 9	yes	2758 ± 9	2716 ± 39	2715 ± 37
$\alpha_s(M^2_Z)$	–	yes	0.1194 ± 0.0029	0.1194 ± 0.0029	0.1194 ± 0.0028

Input values and fit results for the observables used in the global electroweak fit.

Top-quark pole mass from tt-bar+1 jet

The m_t^{pole} dependence of the $t\bar{t} + 1$-jet cross section ($\sigma_{t\bar{t}+1\,\text{jet}}$) is enhanced:

$$\frac{\Delta\sigma_{t\bar{t}+1\text{-jet}+X}}{\sigma_{t\bar{t}+1\text{-jet}+X}} \approx -5 \frac{\Delta m_t^{pole}}{m_t^{pole}} \Rightarrow \text{from NLO calculations}\ \text{[JHEP 10 (2015) 121]}$$

The pole mass can be extracted from: the normalized differential distribution

$$R\left(m_t^{pole}, \rho_s\right) = \frac{1}{\sigma_{t\bar{t}+1\text{-jet}+X}} \frac{d\sigma_{t\bar{t}+1\text{-jet}+X}}{d\rho_s}\left(m_t^{pole}, \rho_s\right), \quad \rho_s = \frac{2m_0}{\sqrt{s_{t\bar{t}j}}} \dashrightarrow \boxed{170\ \text{GeV}}$$

A template technique is used to extract m_t^{pole}.

ATLAS: measured top-quark pole mass (7 TeV, L=4.6fb^{-1}):

> Selection: ℓ+jets ($\ell = e$ or μ) with two b-tags
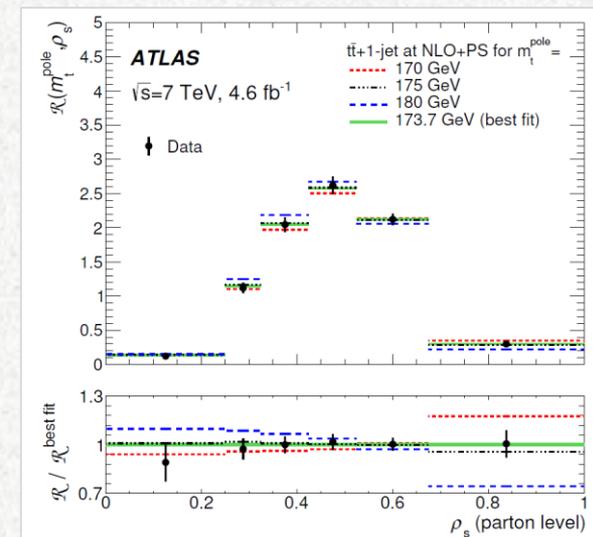> Background: Single top, W/Z+jet, fake leptons,...

$$m_t^{\text{pole}} = 173.7 \pm 1.5\,(\text{stat.}) \pm 1.4\,(\text{syst.})\, {}^{+1.0}_{-0.5}(\text{theory})\ \text{GeV}$$

Systematics: μ_R, μ_F variation, JES, ISR/FSR, PDF

CMS: similar analysis based on observable ρ_s in *dilepton channel* at 8 TeV, L=19.7fb^{-1} [TOP-13 -006]:

$$m_t^{\text{pole}} = 169.9 \pm 1.1\,(\text{stat.})\, {}^{+2.5}_{-3.1}(\text{syst.})\, {}^{+3.6}_{-1.6}(\text{theory})\ \text{GeV}$$

Systematics: μ_R, μ_F variation, jet-parton matching, hadronization, color reconnection

Top quark mass template method

Basic idea of the template method - ℓ+jets topology :

✓ to find invariant mass of top decay products: $t \to bq\bar{q}, \bar{t} \to \bar{b}l\nu, \ t \leftrightarrow \bar{t}$

✓ Using reconstructed objects of candidate events a kinematic fitter is used to find 4-momenta of top decays products .

✓ Kinematic fitter minimizes χ^2 function, e.g.:

$$\chi^2 = \sum_{i=l,4\,jets} \frac{\left(p_T^{i,fit} - p_T^{i,meas}\right)^2}{\sigma_i^2} + \sum_{j=1.2} \frac{\left(U_j^{fit} - U_j^{meas}\right)^2}{\sigma_j^2} + \frac{\left(M_{jj} - M_W\right)^2}{\Gamma_W^2} + \frac{\left(M_{l\nu} - M_W\right)^2}{\Gamma_W^2} + \frac{\left(M_{bjj} - m_t^{rec}\right)^2}{\Gamma_t^2} + \frac{\left(M_{bl\nu} - m_t^{rec}\right)^2}{\Gamma_t^2}$$

Problem: for candidate event we can have several event configurations – connected with different assignments of jets to quarks - without b-tagging: 12 configurations per a LJ event (and for 1 or 2-btags?)

✓ The χ^2 fit is applied to all the event configurations

✓ KF gives for each event combination m_t^{rec} and χ^2 - the correct $m_t^{rec} \Leftrightarrow$ minimal χ^2

Using MC for a given input top mass - expected rec. mass distribution (template) can be found – data mass distr. is compared with mass templates

The Profile Likelihood Approach

$$L(\mu, \vec{\theta}) = \prod_i Pois(d_i | \mu S(\vec{\theta}) + B(\vec{\theta})) \prod_n Gaus(t_n = 0 | \theta_n, \sigma_{t_n} = 1)$$

bins

Poisson probability distribution

data yields

signal strength (POI)

signal prediction

background prediction

uncertainty in auxiliary measurement / "pre-fit uncertainty" on NP

All the **systematic uncertainties** taken into account in the **likelihood** by means of **constrained nuisance parameters (NPs)**

- ○ **constraint terms**: simplified version of auxiliary measurements of NPs (calibrations)
- ○ single fit → best-fit value and total uncertainty in the parameter of interest (POI)
- ○ as a by-product → best-fit values and uncertainties for NPs:
  - ■ "**shifts**" (or, inappropriately, "pulls"): **(θ - t) / σ_t**
  - ■ "**constraints**": σ_θ / σ_t